**RAA 2016** Vol. **16** No. **6**, 98 (6pp) doi: 10.1088/1674–4527/16/6/098
*http://www.raa-journal.org* *http://iopscience.iop.org/raa*

***R**esearch in*
***A**stronomy and*
***A**strophysics*

# Preliminary numerical simulation of mirror seeing for the Chinese Future Giant Telescope

En-Peng Zhang[1,2], Xiang-Qun Cui[3], Guo-Ping Li[3], Yong Zhang[3], Jian-Rong Shi[1,2] and Yong-Heng Zhao[1,2]

[1] National Astronomical Observatories, Chinese Academy of Sciences, Beijing 100012, China; *zhangep@bao.ac.cn*
[2] Key Laboratory of Optical Astronomy, Chinese Academy of Sciences, Beijing 100012, China
[3] Nanjing Institute of Astronomical Optics and Technology, National Astronomical Observatories, Chinese Academy of Sciences, Nanjing 210042, China

Received 2015 December 16; accepted 2016 January 25

**Abstract** Mirror seeing will be one of the key factors influencing image quality of an extremely large ground-based optical telescope (ELT). Computational fluid dynamics (CFD) can be used to estimate the mirror seeing and the effects of ventilation. In this paper, we present a simplified approach to simulation of mirror seeing for the Chinese Future Giant Telescope (CFGT, 30 m in diameter) with the CFD software ANSYS Icepak. We get the FWHM of the image and the distribution of refractive index structure function ($C_{\rm N}^2$) above the mirror. We demonstrate that thermal control and ventilation are effective ways to improve the image quality. Our simulation results agree with those of other authors for the ELT. To reduce the mirror seeing to a level of $0.5''$, the suggested temperature excess of the primary mirror above the ambient air for thermal control of the CFGT is $0-2$ K according to the present results of weakly forced convection. The limitations of the method are also discussed.

**Key words:** astronomical instrumentation — methods: numerical — telescopes

## 1 INTRODUCTION

The image quality of an extremely large ground-based optical telescope (ELT) is limited by site seeing, dome seeing and mirror seeing. It is widely accepted that mirror seeing is caused by atmospheric turbulence in a thin region over the mirror, which is warmer than ambient air (Zago 1997). However, there are very limited measurements of mirror seeing. Laboratory studies of the effects of mirror seeing have been performed by several researchers. In 1979, Lowne gave a quantitative assessment of mirror seeing with a 254 mm spherical mirror. He also studied the effects of inclination and forced air blowing (Lowne 1979). Iye et al. evaluated the seeing degradation using a 62 cm active optics telescope model with and without forced air convection (Iye et al. 1991). Zago gave empirical relations for mirror seeing under natural and forced convection (Zago 1997). For free or natural convection, he derived the expression

$$\theta = 0.38\Delta T^{1.2}. \quad (1)$$

For forced convection, he gave

$$\theta = 0.18\left(\frac{g}{T_{\rm ref}}\right)^{1.3} D^{0.3}\Delta T^{1.3}U^{-0.6}. \quad (2)$$

In Equation (2) ($\theta$-$\Delta T$-$U$ relation), $\theta$ is the angular size of an image (Full Width at Half Maximum (FWHM)) in arcsec, $\Delta T$ is the temperature difference between the mirror and the ambient air in K, $g$ is the gravitational acceleration, $T_{\rm ref}$ is the reference temperature in K, $D$ is the mirror diameter in m and $U$ is the air velocity above the mirror in m s$^{-1}$. The above relations agree well with experiments using small size telescopes. However, whether the formula is applicable for larger telescopes, especially an ELT, still needs to be evaluated.

With the development of science and technology, the aperture size of "the biggest telescope in the world" has increased by three orders of magnitude over the past 400 years. As the size of a monolithic mirror for ground-based telescopes is limited to about 8 m, a segmented primary mirror is a good option for a larger telescope. Future ELTs will range in size between 20 and 100 m. For example, the Thirty Meter Telescope (TMT) will be the first next generation ELT that is scheduled to be constructed and the proposed European Extremely Large Telescope (E-ELT) has an even larger mirror that is 39 m in diameter.

The success of the Large Sky Area Multi-Object Fiber Spectroscopic Telescope (LAMOST) demonstrates that Chinese scientists and engineers have the capability of building an ELT. LAMOST, also called the Guo Shou Jing

Telescope) represents a giant step for Chinese astronomy. It combines thin deformable mirror active optics with segmented active optics. Its primary mirror (Mb, 6.67 m $\times$ 6.05 m) and active Schmidt mirror (Ma, 5.74 m $\times$ 4.40 m) are both segmented. It has an innovative active reflecting Schmidt configuration which continuously changes the mirror's surface during the observation process (Cui et al. 2012). LAMOST provides a new window on the universe for astronomers that is rich in scientific discoveries. Chinese astronomers hope to build a much larger telescope in the future. In fact, Chinese scientists have already investigated the configuration of an ELT ($30 - 100$ m in diameter) (Su et al. 2000, Su et al. 2004a, Su et al. 2004b, Li & Yang 2004). According to their preliminary design, the Chinese Future Giant Telescope (CFGT) will be a 30 m telescope with a segmented primary mirror consisting of 1122 submirrors arranged in 17 rings.

The effect of mirror seeing is possibly hidden in the background seeing associated with a particular site or dome seeing for a given telescope. However, as the ELT will be constructed at a good site and housed in a dome designed to optimize seeing, the mirror seeing could be the main contribution to seeing in the ELT. Problems with mirror seeing would make it hard to achieve the scientific goals.

LAMOST is located at Xinglong Observing Station, administered by National Astronomical Observatories, Chinese Academy of Sciences (NAOC) and the site seeing is about $2''$ (Cui et al. 2012). To improve the performance of LAMOST, many attempts have been made to reduce the dome seeing and mirror seeing during the design, construction and commissioning process. The image quality has been improved significantly since the pilot survey started in October, 2011. However, the site seeing of Xinglong will limit the performance of the LAMOST even when dome and mirror seeing have been reduced to acceptable levels. The CFGT, as well as other ELTs, will address some of the most prominent or fundamental questions in astrophysics such as the nature of dark matter and dark energy, the formation of the first stars and first galaxies, exoplanets and signs of life on them, and so on. To assure its competitiveness, the CFGT or the successor to LAMOST should be placed at one of the best sites in the world. At that time, the issue of mirror seeing will become more prominent. So, a preliminary study of mirror seeing is very important before the ELT is designed or built. Numerical simulation of mirror seeing with appropriate software will provide a powerful and fast method to address for this issue.

The effect of seeing can be understood from the standpoint of computational fluid dynamics (CFD). A numerical CFD model can be used to compute the mean seeing effect along a given line of sight. Vogiatzis & Upton (2006) (VU06) simulated mirror seeing for the TMT. In 2004, Hao et al. simulated the temperature distribution in the dome for the LAMOST project with CFD software (ANSYS Icepak) (Hao 2004). It is necessary to investigate the application of ANSYS Icepak in predicting mirror seeing for the CFGT or the successor of LAMOST.

In this paper, we give our preliminary simulation of mirror seeing for the CFGT (30 m in diameter) using ANSYS Icepak in cases of (weakly) forced convection. The rest of the paper is organized as follows. In Section 2, we describe the theoretical background, the CFGT model and the simulation results. In Section 3, we give the summary and discussion.

## 2 THEORETICAL AND NUMERICAL APPROACHES

### 2.1 Theoretical background

In turbulence theory developed by Kolmogorov and Obhukov, kinetic energy injected into the atmosphere leads to temperature and refractive index fluctuations. The refractive index ($N$) of air can be expressed using Cauchy's (or the Cauchy-Lorenz) formula (Zago 1997)

$$N - 1 = \frac{77.6 \times 10^{-6}}{T}\left(1 + 7.52 \times 10^{-3}\lambda^{-2}\right) \times\left(P + 4810\frac{v}{T}\right), \quad (3)$$

where $T$ is the temperature in units of K, $\lambda$ is wavelength, $P$ is pressure in mb and $v$ is water vapor pressure in mb. In the inertia subrange, Tatarskii (1961) gave the temperature structure function as

$$D_{\rm T}(\Delta r) = C_{\rm T}^2(\Delta r)^{2/3}, \quad (4)$$

where $\Delta r$ is the separation and $C_{\rm T}^2$ is the "temperature structure coefficient."

The refractive index structure function, $C_{\rm N}^2$, is related to $C_{\rm T}^2$ as

$$C_{\rm N}^2 = C_{\rm T}^2\left[77.6{\times}10^{-6}(1 + 7.52{\times}10^{-3}\lambda^{-2})\frac{P}{T^2}\right]^2. \quad (5)$$

Tatarskii (1961) also related $C_{\rm T}^2$ to the dissipation rate of turbulent kinetic energy ($\varepsilon$) and the temperature dissipation rate ($\varepsilon_\theta$) in the inertia domain (Zago 1997)

$$C_{\rm T}^2 = a^2\varepsilon_\theta\varepsilon^{-1/3}, \quad (6)$$

where $a^2 \sim 3$ and

$$\varepsilon_\theta = \kappa_{\rm t}\left(\frac{\partial T}{\partial x_k}\right)^2, \quad (7)$$

$$\varepsilon = \frac{1}{2}\nu_{\rm t}\left(\frac{\partial u_i}{\partial x_k} + \frac{\partial u_k}{\partial x_i}\right)^2. \quad (8)$$

In the above expressions, $\nu_{\rm t}$ is the turbulent viscosity, $\kappa_{\rm t}$ is the equivalent coefficient of turbulent thermal diffusion and $u_i$ are the wind velocity ($U$) components ($i = 1, 2, 3$).

The Fried parameter $r_0$ is given by

$$r_0 = 0.184\lambda^{6/5}(\cos\gamma)^{3/5}\left[\int_0^z C_{\rm N}^2(z)dz\right]^{-3/5}, \quad (9)$$

where $\gamma$ is the zenith angle. We get the FWHM of the image

$$\theta = 0.98\lambda/r_0. \quad (10)$$

With Equations (5), (6), (9) and (10), we establish the relation between FWHM of the image and quantities related to fluid dynamics and turbulence theory.

In ANSYS Icepak, the effects of turbulence can be modeled through the $k-\varepsilon$ approximation ($k$ is turbulent kinetic energy). We can get $\nu_{\rm t}$ with the output variables $k$ and $\varepsilon$ in the simulation results

$$\nu_{\rm t} = C_\mu \frac{k^2}{\varepsilon}, \quad (11)$$

where $C_\mu$ ($= 0.09$) is an empirical constant in the software. The turbulent thermal diffusion, $\kappa_{\rm t}$, is given by $Pr_{\rm t} = \nu_{\rm t}/\kappa_{\rm t}$. $Pr_{\rm t}$ is the turbulent Prandt number, which has been set to 0.85 in the software. In principle, we can calculate image size $\theta$ by deriving $\nu_{\rm t}$, $\kappa_{\rm t}$ and distributions of $U$ and $T$ with ANSYS Icepak.

### 2.2 The CFGT model

The structure of CFGT is still being optimized. The approximate size of a submirror is about 0.8 m × 0.8 m and the thickness may be less than 100 mm. In this paper, the model of the CFGT primary mirror is a cylindrical plate with diameter $D = 30$ m and thickness $H = 0.04$ m. We neglect the hole with diameter 2.8 m at the center of the primary mirror which was designed in Su et al. (2004b). The computational region should be large enough to ensure that the global wind field is parallel to the top surface of the plate. The computational time should be long enough to guarantee that the value of the output variables such as $P$, $T$ and so on do not change with time.

Figure 1 shows a representative plot of the CFGT model. First, we adopt similar parameters to those of VU06 for checking our method. The ambient air temperature is $T_0 = 273$ K and atmospheric pressure is $P_0 = 1000$ mb. Wind speed $\sim U = 0.5$ m s$^{-1}$ is considered and the gravitational acceleration is $g = 9.80665$ m s$^{-2}$ in the software. The wavelength in Equation (10) is $\lambda = 0.5$ μm and the mirror temperature is $T_{\rm m} = 273.1$ K. The error tolerance for continuum and energy equations are set to $10^{-3}$ and $10^{-7}$, respectively.

As $\Delta T\,(= T_{\rm m} - T_0)$ is small, we take the reference temperature as $T_{\rm ref} = T_0$ and reference ambient pressure $P_{\rm ref} = P_0$ for simplification. We also neglect radiation heat transfer due to small $\Delta T$ in forced convection. From Equation (5), we get

$$C_{\rm N}^2 = C_{\rm T}^2\left[7.8\times10^{-5}\frac{P_{\rm ref}}{T_{\rm ref}^2}\right]^2. \quad (12)$$

As the wind is parallel to the plate, Equation (7) can be reduced to the one dimensional form

$$\varepsilon_\theta \approx \kappa_{\rm t}\left(\frac{dT}{dz}\right)^2. \quad (13)$$

We rewrite Equation (10) as

$$\theta = 5.25\times2.06\times10^5\lambda^{-1/5}\left[\int_0^z C_{\rm N}^2(z)dz\right]^{3/5}, \quad (14)$$

where $\cos\gamma = 1$. The interval of integration is chosen as $z \in [0-30]$ cm. The Richardson number is $R_{\rm i} = \frac{g}{T_{\rm ref}}\left(\frac{dT}{dz}\right)\left(\frac{dU}{dz}\right)^{-2}$ and $R_{\rm i} \ll 10$ is required.

### 2.3 Simulation Results and Comparison

Figure 2 shows a representative plot of the $C_{\rm N}^2$ as a function of perpendicular distance ($z$) from the plate at $x = 14.6$ m for $\Delta T = 0.1$ K and $U = 0.5$ m s$^{-1}$. We also plot data estimated from VU06. We estimate mirror seeing with another expression of $C_{\rm T}^2$ using the Monin-Obukhov length ($L$) (Zago 1997)

$$C_{\rm T}^2 = 4.9\,(1-7z/L)^{-2/3}\left(q/u_*\right)^2 z^{-2/3}, \quad (15)$$

where $L = -\frac{u_*^3 T}{k_{\rm a} g q}$, $u_*$ is the friction velocity, $q$ is the surface temperature flux, $k_{\rm a} \sim 0.4$ is the Karmann constant and $z$ is the distance above the surface of the ELT plate.

Table 1 gives the mirror seeing estimated from different methods or expressions for $\Delta T = 0.1$ K and $U = 0.5$ m s$^{-1}$. They agree with each other considering the different software, methods and mesh schemes used. We have pointed out that Equation (2) ($\theta$-$\Delta T$-$U$ relation) is derived by considering a small size mirror. We do not know if it is applicable for an ELT. For the TMT, VU06 gave a dimensional analytical relation as

$$\theta \prec l^{18/105}\Delta T^{1.2}U^{-3/105}, \quad (16)$$

where $l = (x + 15)$ (Fig. 2). As the index of $U$ in Equation (16) is much less than that of Equation (2), the seeing changes much faster with wind speed when calculated with Equation (2) (See also Table 2).

We note that there are some differences in the $C_{\rm N}^2$ profile when the height $z > 0.14$ m in Figure 2. The trend of our line agrees with the "MO" line (Eq. (15)) very well. We also note that Equation (15) was derived from the study of turbulence structure over a flat, unobstructed plain in Kansas (Wyngaard et al. 1971). However, it is used to estimate mirror seeing of a finite size plate. So, the uncertainties associated with this method need further study. Similar to VU06, we just take the $\theta$ at $x = 14.6$ m as the characteristic value of mirror seeing for simplification considering the edge effect at $x = 15$ m. In fact, $\theta$ changes with $x$ very slowly as $\theta \prec l^{18/105}$ in Equation (16).

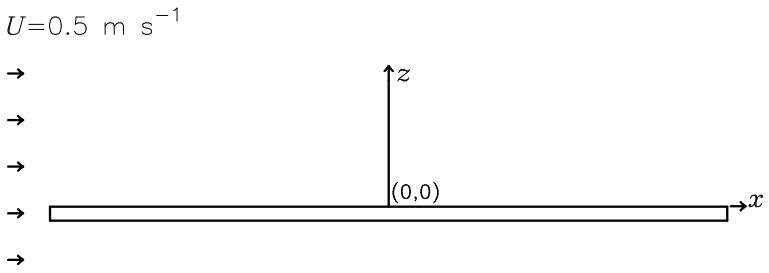


**Fig. 1** Simplified CFD model of the CFGT. Wind speed $U = 0.5$ m s$^{-1}$. Here we only plot the central cross section and $x \in [-15, 15]$ m.

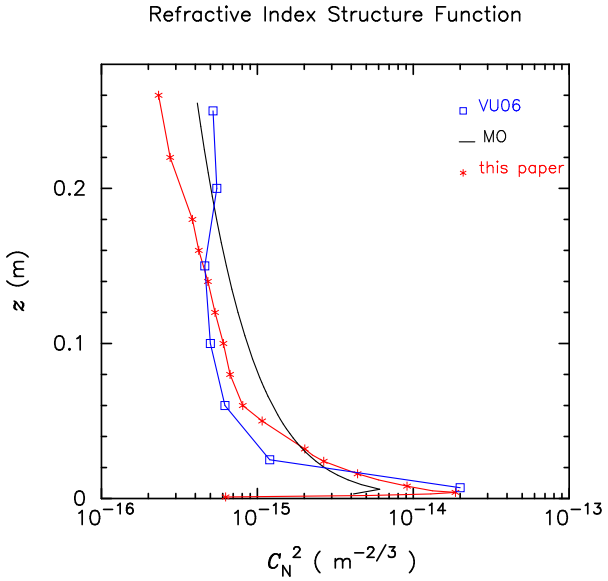


**Fig. 2** $C_{\rm N}^2$ distributions above the CFGT model at $x = 14.6$ m for $\Delta T = 0.1$ K and $U = 0.5$ m s$^{-1}$. VU06: data estimated from VU06; MO: data estimated by the Monin-Obukhov length; this paper: simulation results of this paper.

**Table 1** Mirror Seeing Estimated from Different Methods ($\Delta T = 0.1$ K and $U = 0.5$ m s$^{-1}$).

| Methods | This paper | MO | VU06 | Eq. (2) |
|---|---|---|---|---|
| Mirror seeing (arcsec) | 0.016 | 0.011 | 0.012 | 0.014 |

Notes: MO – data estimated by the Monin-Obukhov length ($L$).

To examine the effect of ventilation under different $\Delta T$, we simulate the cases of $U = 0.5, 1.5$ m s$^{-1}$ and $\Delta T = 1.0, 2.0$ K for the CFGT. We still consider $T_0 = 273$ K and $P_0 = 1000$ mb for comparison.

Table 2 and Figure 3 show mirror seeing of the CFGT at different temperature differences and wind speeds. We also give the $\theta$ estimated with Equation (2) derived for a small size telescope in Table 2. The index of $U$ is $-0.6$ in Equation (2) while it is $-3/105$ in Equation (16). We can see that $\theta$ decreases faster than the simulation result. (It can be seen from the ratio of $\theta_{\rm U=1.5}/\theta_{\rm U=0.5}$ for each method with the same $\Delta T$). Our present simulation results qualitatively favor Equation (16) rather than Equation (2). Further study, especially real observations, should be conducted to test the dependence of $\theta$ on $U$ for an ELT.

For $U = 0$ m s$^{-1}$ and $\Delta T = 2.0$ K, the mirror seeing of the CFGT is $\sim 0.87''$ according to Equation (1). We can see that an effective way to reduce the effect of mirror seeing is through temperature control and ventilation. Theoretically, increasing wind flushing will decrease mirror seeing more efficiently. However, considering wind buffeting, there should be an optimal wind speed. This is-

**Table 2** Simulation of Mirror Seeing for Different $\Delta T$ (K) and $U$ (m s$^{-1}$)

| | $\Delta T = 1.0$ | $\Delta T = 2.0$ |
|---|---|---|
| $U = 0.5$ | $0.25''$ ($0.28''$) | $0.6''$ ($0.69''$) |
| $U = 1.5$ | $0.2''$ ($0.14''$) | $0.5''$ ($0.35''$) |

Notes: The values in the parentheses are seeing estimated by Equation (2).

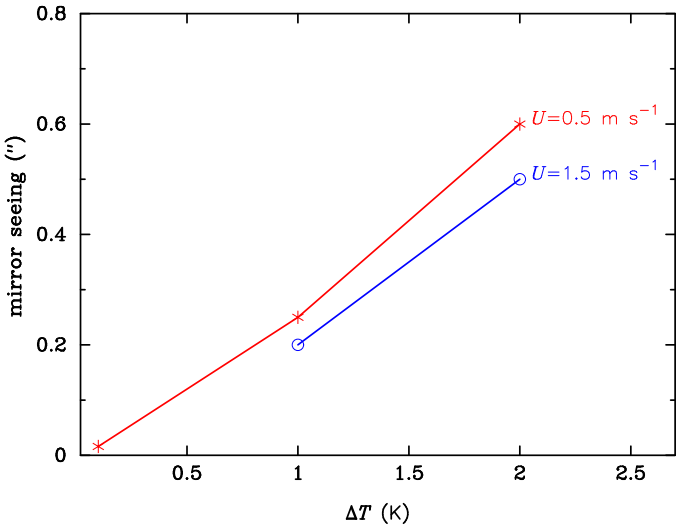


**Fig. 3** Mirror seeing estimated for the CFGT model at $x = 14.6$ m for different $U$ and $\Delta T$.

sue is out of the scope of this paper and we will address the case of larger $U$ in future work. We will also simulate natural convection in a future study.

Racine et al. (1991) published a value of $0.43''$ for the median atmospheric seeing at the CFHT site, with the 10th and 90th percentiles being $\sim 0.25''$ and $\sim 0.7''$, respectively. So, the suggested temperature difference for thermal control of the CFGT primary mirror is $0 - 2$ K if it were placed in as good a site as Mauna Kea with a wind speed of $1 - 2$ m s$^{-1}$ according to the present simulation results.

Figure 3 and Table 2 show that it is even more important to reduce the temperature difference to decrease mirror seeing. There are many methods for reducing the temperature difference between the mirror and the ambient air such as reducing heat generated by actuator going into the segments, reducing the thermal inertia of the submirror, ventilation and so on.

## 3 SUMMARY AND DISCUSSION

Mirror seeing is one of the key factors affecting the image quality of the ELT. Avoiding mirror seeing is an important issue in the design and construction of an ELT. CFD can provide a useful theoretical structure for understanding and controlling the phenomenon of mirror seeing in telescopes.

In this paper, we present our simplified approach of simulating mirror seeing for the CFGT in cases of weakly forced convection. We calculate the FWHM of the image and the distribution of $C_{\rm N}^2$, especially in the region $z = 0 - 7$ mm above the mirror which is lacking in VU06. We demonstrate that an effective way to improve the image quality is through mirror temperature control and ventilation. We also compared our results with VU06 and the associated empirical relations. We give a preliminary suggestion for the temperature difference and air velocity that are applicable for thermal control of the CFGT primary mirror under good site seeing. These results are helpful for the design of CFGT and will be refined in a future study. In addition, we showed that ANSYS Icepak can be used to estimate the mirror seeing of an ELT.

There are limitations to the method presented in this paper in estimating mirror seeing. First of all, the model of CFGT is a monolithic plane mirror. However, the real CFGT must be segmented and spherical. We do not consider the variation of temperature on the plate due to wind flushing and heat transfer from the actuator. Equation (13) is only applicable to a steady state situation. A more realistic model should be used in a future simulation. We also note that there are many turbulence models, simulation methods and commercial CFD software available. We do not know whether the simulation results depend heavily on the software. The simulation results should be compared with future observed data to test the model and the method.

**Acknowledgements** The authors gratefully acknowledge the support of the Large Scientific Equipments Repairing Project of Chinese Academy of Sciences: “Cooling Facility and Monitoring instruments for LAMOST Dome Seeing Improvement”.

## References

Cui, X.-Q., Zhao, Y.-H., Chu, Y.-Q., et al. 2012, RAA (Research in Astronomy and Astrophysics), 12, 1197

Hao, W.-N. 2004, PhD Thesis (*http://ir.niaot.ac.cn/handle/114a32/701*)

Iye, M., Noguchi, T., Torii, Y., Mikami, Y., & Ando, H. 1991, PASP, 103, 712

Li, G., & Yang, D. 2004, in Proc. SPIE, 5495, Astronomical Structures and Mechanisms Technology, eds. J. Antebi & D. Lemke, 204

Lowne, C. M. 1979, MNRAS, 188, 249

Racine, R., Salmon, D., Cowley, D., & Sovka, J. 1991, PASP, 103, 1020

Su, D.-Q., Cui, X., Wang, Y.-N., & Wang, S.-G. 2000, in Proc. SPIE, 4004, eds. T. A. Sebring & T. Andersen, 340

Su, D.-Q., Wang, Y.-N., & Cui, X.-Q. 2004a, Chinese Astronomy and Astrophysics, 28, 356

Su, D.-Q., Wang, Y.-N., & Cui, X. 2004b, in Proc. SPIE, 5489, ed. J. M. Oschmann, Jr., 429

Tatarskii, V. I. 1961, Wave Propagation in Turbulent Medium (McGraw-Hill)

Vogiatzis, K., & Upton, R. 2006, in Proc. SPIE, 6271, Society of Photo-Optical Instrumentation Engineers (SPIE) Conference Series, 627115

Wyngaard, J. C., Izumi, Y., & Collins, Jr., S. A. 1971, Journal of the Optical Society of America (1917–1983), 61, 1646

Zago, L. 1997, in Proc. SPIE, 2871, Optical Telescopes of Today and Tomorrow, ed. A. L. Ardeberg, 726